Generalized Chimera States in Two Interacting Populations of Kuramoto Oscillators

A RESEARCH PROJECT
SUBMITTED TO THE DEPARTMENT OF MATHEMATICS,
OF THE UNIVERSITY OF MINNESOTA DULUTH
BY

Soleh K Dib

IN PARTIAL FULFILLMENT OF THE REQUIREMENTS
FOR THE DEGREE OF
MASTER OF SCIENCE

Dr. Bruce Peckham

2016

Acknowledgements

First and foremost I would like to thank my advisors past and present, Dr.s Bruce Peckham and Dalibor Froncek, who have both been indispensable to my academic success. I would also like to thank my family, friends, and the Department of Mathematics at UMD in general, and all the fine professors from whom I have learned in these past many years here.

Abstract

An important class of problems in the field of dynamical systems considers networks of oscillators, each of which effects the others. Commonly in considering such systems the concern is whether or not these oscillators will evolve into a state of synchrony. The Kuramoto model consists of "limit-cycle" oscillators (meaning that each is described only in terms of its angle of revolution on a circle), all coupled to each other through a common, time independent function of the phase variables.

In 2002 it was discovered that systems of coupled identical oscillators can in fact exhibit states in which a sub-population of oscillators fully clusters (attains "phase-synchrony") while the remainder do not. Shortly thereafter, Abrams, Strogatz, Mirollo and Wiley proposed a simple, solvable variation on the Kuramoto model which contains such "Chimera" states.

For our research we generalize the concept of a chimera state to the case that the traditionally fully clustered state is allowed to be in a constant state of partial clustering. We characterize the conditions under which a generalized chimera exists as a persistent state for this same variant on the Kuramoto model, finding that it is a rare phenomenon, requiring much stricter conditions than for the traditional chimera.

Contents

List of Figures

Chapter 1

Introduction

The collective synchronization or desynchronization of what may be modeled as networks of coupled oscillators is a phenomenon which appears in many fields of science, from crickets chirping in unison to pacemaker cells synchronizing in the brain; from arrays of superconducting Josephson Junctions to grandfather clocks resting on an imperfectly rigid surface. In many cases this synchronization takes place despite the fact that the individual oscillators have varying natural frequencies of oscillation. While this is what initially generated interest in examining collective synchronization, there have since developed many interesting aspects of the coupled oscillator problem which do not depend on any variation in natural frequency across the population. It is this case of "identical" oscillators which we will consider in this paper.

1.1 The Kuramoto Model

In 1975 Kuramoto proposed his eponymous model of limit cycle phase coupled oscillators which has come to be the standard model in the field. It is shown to be a limiting case of several types of then studied models, maintaining many interesting aspects of the behaviour of those models while being simple enough to admit analytic attacks [1].
The basic Kuramoto model is defined by a constant, universal coupling strength acting on sines of the phase differences of the oscillators. The uniform nature of the coupling strength coefficient earns this original version of the model the label "globally coupled"

- a theme which has been expanded on significantly since its inception. Each oscillator generally has an individual natural frequency ω_i, with the model being defined by the system of N equations:

$$\dot{\theta}_i = \omega_i + \frac{K}{N}\sum_{j=1}^{N}\sin(\theta_j - \theta_i) \quad i = 1, 2, \ldots, N \tag{1.1}$$

with $\theta_i \in [0, 2\pi)$. For this research we will employ a common generalization of this model in which there is included a constant, global "phase lag" term α within the argument of the sine functions. As mentioned, we will also restrict our attention to populations of identical oscillators - that is, populations of oscillators which share a common natural frequency ω. We may, and do, choose to measure the phase of each oscillator relative to an arbitrary rotating reference frame. Specifically we will measure them relative to the frame rotating at the rate ωt, resulting in the transformation

$$\theta_i \to \theta_i - \omega t$$

which, for identical oscillators, removes the natural frequency term from the system of equations (1.1) entirely.

Note that in the case of identical oscillators we may rescale time to absorb any non-zero constant factor common to each of the system equations without altering the structure of the system equations. We take advantage of this to scale out the coupling strength coefficient K (we will find it advantageous to retain the population size scaling factor $1/N$), employing the time transformation $t \to Kt$. Note that the case $K = 0$ need not generally be considered as it results in the trivial system of disconnected oscillators, in which case they each revolve at a constant velocity. The Kuramoto model with identical oscillators and a constant phase lag term can thus be represented in its full generality by the system

$$\dot{\theta}_i = \frac{1}{N}\sum_{j=1}^{N}\sin(\theta_j - \theta_i - \alpha) \quad i = 1, 2, \ldots, N \tag{1.2}$$

Note that the transformation $\alpha \to \alpha + \pi$ simply introduces a factor of -1 to each equation, and so is equivalent to the transformation $t \to -t$. As the model is invariant up to time scale under these transformations, we may thus restrict our attention to the parameter space $-\frac{\pi}{2} < \alpha \leq \frac{\pi}{2}$. We may in fact restrict this space further by taking advantage of the reflection symmetry of the model: the system (1.2) is invariant under the combined transformation $\theta_i \to -\theta_i, \alpha \to -\alpha$. Thus we may, without loss of generality,

restrict ourselves to the parameter space $0 \leq \alpha \leq \frac{\pi}{2}$.

Even under the simplifying assumption that the oscillators have identical natural frequencies $\omega_i = \omega$ the determination of all possible trajectories of this system and the stability of those states is non trivial.

It is possible to completely solve the system for two oscillators by employing the transformation $\psi = \theta_1 - \theta_2$, resulting in the one dimensional system

$$\dot{\psi} = -\sin(\psi)\cos(\alpha)$$

This system has a stable equilibrium in ψ-phase space at $\psi = 0$ (since $\cos(\alpha) > 0$) and an unstable equilibrium at $\psi = \pi$, unless $\alpha = \pi/2$ in which case every point in ψ-phase space is a neutrally stable equilibrium. With any non zero coupling strength, and $\psi(0) \neq \pi$ the oscillators tend toward $\psi = 0$, and thus become "phase-locked", in which $\theta_1 = \theta_2$, both occupying the same position on the circle. If instead $\psi(0) = \pi$ the oscillators will of course remain in this unstable equilibrium. Thus for all cases the long term behaviour is $\psi(t) = \psi_0$ for some constant ψ_0 (not necessarily the initial value). Since ψ - the difference in angular position of the two oscillators, $\theta_1 - \theta_2$ - is constant the two oscillators are in a "frequency locked" state, meaning that $\dot{\theta}_1 = \dot{\theta}_2$.

With three oscillators the problem becomes slightly more challenging, but is still solvable. Utilizing the change of variables

$$\psi = \theta_1 - \theta_2, \quad \phi = \theta_1 - \theta_3$$

reduces the model to a two dimensional system of equations allowing all outcomes to be described via a stability analysis of the equilibrium solutions. We note that these equilibria are only constant in ψ and ϕ: the original phase variables θ_1, θ_2, and θ_3 are free to vary as long as they do so in a manner which preserves ψ and ϕ. For this system the only possible outcomes are again all frequency locked, with the three oscillators: all in phase ($\psi = 0, \phi = 0$), with two in phase and one frequency locked elsewhere on the circle ($\psi = 0, \phi = \pi$ for $\alpha = 0$), or with all three distributed (evenly, for $\alpha = 0$) around the circle ($\psi = 2\pi/3, \phi = -2\pi/3$ for $\alpha = 0$). The vector field for this system in ψ, ϕ space is pictured in figure 1.1 with $\alpha = 0$. Changing α does not qualitatively change the vector field, but it does change the location of the three saddles which appear, for $\alpha = 0$, at $(\psi, \phi) = (\pi, 0), (0, \pi)$, and (π, π). Note that the sink (at $(0, 0)$) and the sources

(at $(\frac{2\pi}{3}, \frac{4\pi}{3})$ and $(\frac{4\pi}{3}, \frac{2\pi}{3})$) do not move with changes in α.

Beyond $N = 3$, a full characterization of the system becomes difficult, if not impossible.

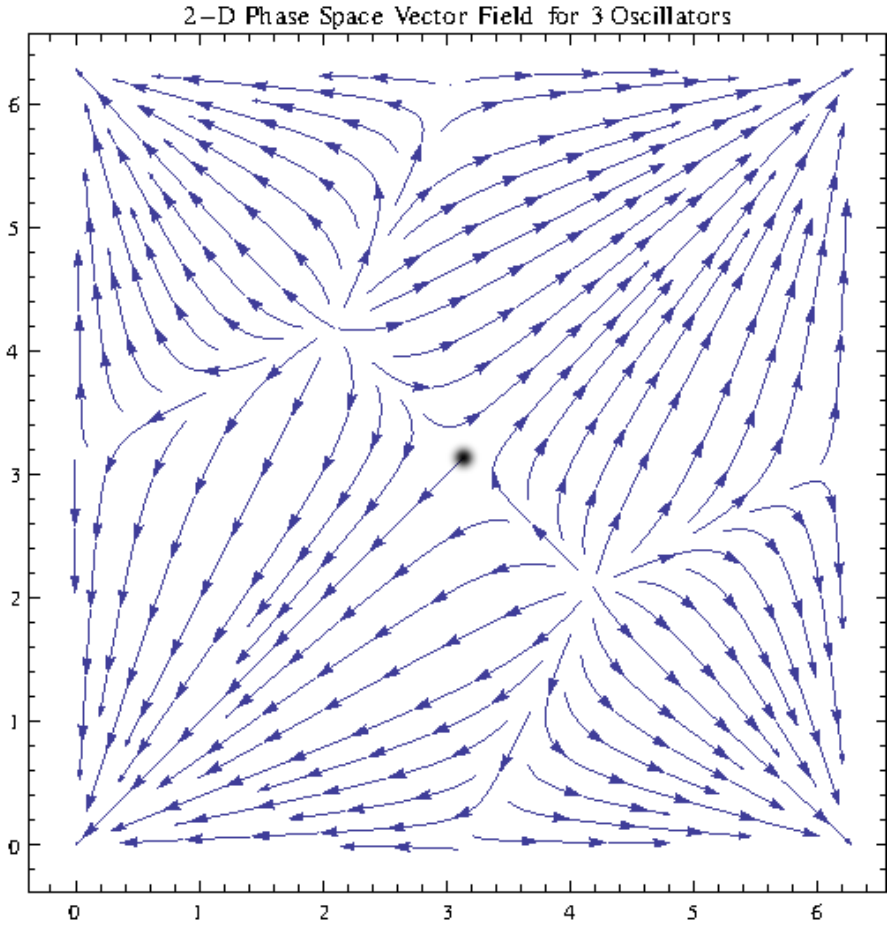

Figure 1.1: Vector Field for Three Oscillators: 2-D Phase Space, ψ vs ϕ

However, in the case of $N > 3$ useful insight may be drawn from the definition of an order parameter which measures the level of clustering in the system. Let the complex order parameter $z(t) = \rho(t)e^{i\phi(t)}$ be defined by

$$z(t) = \frac{1}{N}\sum_{j=1}^{N} e^{i\theta_j(t)} \tag{1.3}$$

One may then express the coupling sine function in our system equations (1.2) as a sum of exponentials, and carry out the sum over $j = 1...N$ and re-sum the exponentials,

restating the system equations in terms of the "order parameter magnitude" ρ and average phase value ϕ,

$$\dot{\theta}_i = \rho \sin(\phi - \theta_i - \alpha) \quad i = 1, 2, \ldots, N$$

While these are not strictly decoupled as $\phi(t)$ and $\rho(t)$ depend on each of the individual θ_i this expression of the model allows us characterize certain interesting classes of behaviour, such as conditions under which the average phase value is constant despite the oscillators being potentially in motion relative to each other.

We will find, however, that much more progress can be made in the limiting case $N \to \infty$, where the order parameter $z(t)$ becomes invaluable. We note, however, that only in the case of $z = 1$ does the order parameter indicate frequency and phase locking. For other values of the order parameter magnitude the oscillators are distributed across an interval of the circle, and potentially in motion relative to each other. From this point on our discussion will focus on the degree of clustering of the population of oscillators - measured by the "order parameter" ρ - rather than whether or not they are phase- or frequency- locked.

1.2 $N \to \infty$ and Dimensional Reduction

In this limiting case we can not speak of "each" oscillator - rather, we describe their position via a distribution function $f(\theta, t)$, describing the density of oscillators at any given phase throughout time. We may then define a velocity equation which generalizes the system equations (1.2) to the $N \to \infty$ case,

$$v(\theta, t) = \int_0^{2\pi} \sin(\theta' - \theta - \alpha) f(\theta', t) d\theta' \tag{1.4}$$

and which must, together with the distribution function, satisfy the continuity condition:

$$\frac{\partial f}{\partial t} = -\frac{\partial}{\partial \theta}(fv) \tag{1.5}$$

Expressing the distribution function $f(\theta, t)$ as a Fourier series in θ (as a probability density function, it is defined to be normalized over a change of 2π in θ at all times t),

$$f(\theta, t) = \frac{1}{2\pi} \sum_{n=-\infty}^{\infty} a_n(t) e^{in\theta} \tag{1.6}$$

and employing the orthogonality of sine and cosine functions over 2π we can complete the integration in (1.4), yielding

$$v(\theta,t) = -\frac{1}{2i}\left[a_1(t)e^{i(\theta+\alpha)} - a_{-1}(t)e^{-i(\theta+\alpha)}\right]$$

Substituting this back into the continuity equation (1.5) and again utilizing orthogonality of sine and cosine we may equate coefficients of each exponential, resulting in the infinity of equations

$$\dot{a}_n(t) = \frac{n}{2}\left[a_{n-1}(t)a_1(t)e^{i\alpha} - a_{n+1}(t)a_{-1}(t)e^{-i\alpha}\right] \tag{1.7}$$

where n ranges from $-\infty$ to ∞.

In 2008 Ott and Antonsen [2] discovered a surprising dimensional reduction via a restriction of the distribution function to a specific invariant manifold. A Poisson Kernel Distribution (PKD) is defined by a Fourier series in which (using the notation of (1.6)) $a_{-n} = a_n^*$ (where $*$ denotes complex conjugation) and $a_n = a(t)^n$ for all $n \geq 0$ and a single coefficient $a(t)$ which then completely defines the distribution. Ott and Antonsen discovered that if at any time $f(\theta,t)$ takes the form of a PKD then the infinity of equations (1.7) are identical for each value of the index n ($n \neq 0$), and thus reduce to one complex evolution equation for $a(t)$. Furthermore, as long as this equation is satisfied the distribution then remains a PKD. That is, let $f(\theta,t)$ take the specific form

$$f(\theta,t) = \frac{1}{2\pi}\left[1 + \sum_{n=1}^{\infty}\left(a^n(t)e^{in\theta} + a^{*n}(t)e^{-in\theta}\right)\right] \tag{1.8}$$

for some complex function of time $a(t)$ expressed in polar coordinates $a(t) = \rho(t)e^{-i\phi(t)}$. Then the evolution of of the n^{th} coefficient of the expansion of f, $a_n = a^n = \rho^n e^{-in\phi}$, is

$$\begin{aligned}
\dot{a}_n(t) &= \frac{\partial}{\partial t}a(t)^n \\
&= \frac{\partial}{\partial t}\left[\rho^n(t)e^{-in\phi(t)}\right] \\
&= n\rho^{n-1}\dot{\rho}e^{-in\phi} - in\rho^n e^{-in\phi}\dot{\phi} \\
&= na^n\left[\frac{\dot{\rho}}{\rho} - i\dot{\phi}\right]
\end{aligned} \tag{1.9}$$

Given that for this form of distribution $a_n = a^n$ and $a_{-n} = a_n^*$ the evolution equations (1.7) become (for $n \geq 1$),

$$\begin{aligned}
\dot{a}_n(t) &= \tfrac{n}{2}\left[a_{n-1}a_1 e^{i\alpha} - a_{n+1}a_{-1}e^{-i\alpha}\right] \\
&= \tfrac{n}{2}\left[a^{n-1}ae^{i\alpha} - a^{n+1}a^* e^{-i\alpha}\right] \\
&= \tfrac{n}{2}\left[a^n e^{i\alpha} - \rho^2 a^n e^{-i\alpha}\right] \\
&= \tfrac{n}{2}a^n\left[e^{i\alpha} - \rho^2 e^{-i\alpha}\right]
\end{aligned}$$

While the case $n = 0$ results in $\dot{a}_0(t) = 0$ in both derivations. Matching these two equations for $\dot{a}_n$ results in the complex differential equation

$$\dot{\rho} - i\rho\dot{\phi} = \frac{1}{2}\rho\left[e^{i\alpha} - \rho^2 e^{-i\alpha}\right]$$

or, in terms of real and imaginary parts,

$$\dot{\rho}(t) = \frac{1}{2}\cos(\alpha)\left[1 - \rho^2\right]\rho \tag{1.10}$$

$$\dot{\phi}(t) = -\frac{1}{2}\sin(\alpha)\left[1 + \rho^2\right] \tag{1.11}$$

If we generalize the order parameter (1.3) to the case of $N \to \infty$ by defining

$$z(t) = \int_0^{2\pi} e^{i\theta} f(\theta, t) d\theta \tag{1.12}$$

and express $f(\theta, t)$ as the Fourier series (1.8) we may easily integrate each exponential term individually to find that $z(t) = a(t)$, and thus the coefficient of the PKD is in fact our order parameter, with $\rho(t)$ measuring the clustering of the oscillators (ranging from zero to one) and $\phi(t)$ measuring the average phase of the population.

The evolution equation for ρ, (1.10), shows that (for $\alpha \neq \pi/2$) all PKD distributions either begin with $\rho = 0$ and remain there or tend towards $\rho = 1$.

In the case $\rho = 1$ the oscillators are phase and frequency locked ("fully clustered"), moving all with the same velocity and in the same position. In terms of the population distribution, we have f as a dirac delta at a position ϕ which moves around the circle with constant velocity $\dot{\phi}(t) = \sin(\alpha)$.

In the case $\rho = 0$ the oscillators are uniformly distributed around the circle. This could be either in parallel to the two (or three) oscillator case in which the oscillators were distributed around the circle and frequency locked, or it could be realized through

uniform random motion. This draws our attention to the fact that we must in general be careful to distinguish between frequency locking and "clustering", meaning a measure of the dispersal of the population around the circle. Frequency locking, in which the oscillators all move with the same rotational velocity, can occur at any level of clustering. Phase locking, in which the oscillators occupy (for all times) the same position on the circle, is equivalent to "full" clustering, and naturally implies frequency locking.

The remaining case, in which $\alpha = \frac{\pi}{2}$, results in the same behaviour as $\rho = 1$, but regardless of the value of ρ.

While Ott and Antonsen subsequently showed that this manifold is globally attracting for a large family of Kuramoto like models [3], they also have shown [4] that it is in fact only neutrally attracting for systems of identical oscillators. That is, if the population distribution is at any point a PKD it will remain so, however, if at any point it is not a PKD it will not be drawn towards one (and is unlikely to become one). Thus, while in the case of identical oscillators this manifold remains invariant, we must recall that any conclusions we draw from subsequent analysis apply only to regions of phase space that lie on the PKD manifold.

1.3 Chimera

Long before the discovery of the Ott and Antonsen ansatz (1.8) it was thought that systems of coupled identical oscillators always behave in a very simple fashion. Systems of non identical oscillators are capable - under the right conditions - of exhibiting a complex behaviour in which part of the population synchronizes (frequency lock) while the remainder continue to wander in a partially dispersed state. It was thought that systems of identical oscillators were not capable of exhibiting this sort of behaviour.

In 2002, however, Kuramoto and Battogtokh discovered [5] that this conventional wisdom was in fact false: that by allowing the coupling coefficient to vary in phase space there were certain initial conditions under which the oscillators did not all exhibit the same behaviour. States in which one sub-population is internally fully clustered while the other is not have been discovered for such systems of identical oscillators, and have been dubbed "Chimera" States.

By 2008 a simple variant on the Kuramoto model with constant coupling strength coefficients was discovered which results in chimerical behaviour [6]. All that is required is to partition the population of oscillators into two sub-groups, each sub-group distributed individually as a PKD (1.8). With one constant coefficient ν describing the inter-group coupling strength, and a separate constant coefficient μ describing the intra-group coupling strength it was found that there are regions of parameter space which admit chimerical solutions for certain subsets of phase space. Specifically, where $\sigma = 1, 2$ is one of the two sub-populations and $\sigma^{'}$ denotes the other, the system equations are

$$\dot{\theta}_i^\sigma = \frac{\mu}{N_\sigma}\sum_{j=1}^{N_\sigma}\sin(\theta_j^\sigma - \theta_i^\sigma - \alpha) + \frac{\nu}{N_{\sigma'}}\sum_{j=1}^{N_{\sigma'}}\sin(\theta_j^{\sigma'} - \theta_i^\sigma - \alpha) \quad i = 1, 2, \dots N_\sigma \tag{1.13}$$

This will be the meaning of super- or sub- scripted σ and $\sigma^{'}$ throughout the remainder of the paper.

In the limiting case $N \to \infty$ each sub-population has its own velocity and continuity equations, as in (1.4) and (1.5):

$$\frac{\partial f^\sigma}{\partial t} = \frac{\partial}{\partial \theta}(f^\sigma v^\sigma) \tag{1.14}$$

$$v^\sigma(\theta, t) = \mu\int_0^{2\pi}\sin(\xi - \theta - \alpha)f^\sigma(\xi, t)d\xi + \nu\int_0^{2\pi}\sin(\xi - \theta - \alpha)f^{\sigma'}(\xi, t)d\xi \tag{1.15}$$

We also define an order parameter as before for each population, and distribute them each according to the ansatz (1.8). That is, for each sub-population σ,

$$f^\sigma(\theta, t) = \frac{1}{2\pi}\left[1 + \sum_{n=1}^{\infty}\left(a_\sigma^n(t)e^{in\theta} + a_\sigma^{*n}(t)e^{-in\theta}\right)\right] \tag{1.16}$$

$$z^\sigma(t) = \int_0^{2\pi} e^{i\theta}f^\sigma(\theta, t)d\theta$$

as in (1.8) and (1.12) respectively. The continuity equations then reduce to the two complex equations

$$\dot{a}_\sigma(t) = \frac{1}{2}\mu\left[a_\sigma(t)e^{i\alpha} - a_\sigma^*(t)a_\sigma^2(t)e^{-i\alpha}\right] + \frac{1}{2}\nu\left[a_{\sigma'}(t)e^{i\alpha} - a_{\sigma'}^*(t)a_\sigma^2(t)e^{-i\alpha}\right] \tag{1.17}$$

or in terms of real and imaginary parts the four ($\sigma = 1, 2$) real equations

$$\dot{\rho}_\sigma(t) = \frac{1}{2}\left[1 - \rho_\sigma^2\right]\left[\mu\rho_\sigma\cos(\alpha) + \nu\rho_{\sigma'}\cos(\phi_{\sigma'} - \phi_\sigma - \alpha)\right] \tag{1.18}$$

$$\rho_\sigma\dot{\phi}_\sigma(t) = \frac{1}{2}\left[1 + \rho_\sigma^2\right]\left[-\mu\rho_\sigma\sin(\alpha) + \nu\rho_{\sigma'}\sin(\phi_{\sigma'} - \phi_\sigma - \alpha)\right] \tag{1.19}$$

We will at this point note that the transformation $\psi = \phi_1 - \phi_2$ will be common throughout this paper, and that we will then be concerned with the three dimensional phase space of ρ_1, ρ_2, and ψ. When we refer to equilibria in general it will be with respect to this space, which does not constrain the original phase variables θ_i or velocity function $v(\theta, t)$ to be constant.

As a fully clustered state for either sub-population σ ($\rho_\sigma = 1$) is an invariant state (1.18), Strogatz et al. were able to completely characterize the chimerical behaviour of the system by assuming (without loss of generality) that $\rho_1 = 1$ and utilizing the transformation $\psi = \phi_1 - \phi_2$ to reduce the system to two dimensions (ρ_2 and ψ). The stability diagram they found for this system, as published in their paper [6] is printed here in figure 1.2. In their paper (we follow their notation in the discussion that follows here) they re-parameterize μ, ν in terms of one parameter, $A = \mu - \nu$ by restricting $\mu + \nu = 1$ through a rescaling of time. Additionally, they use parameter $\beta = \pi/2 - \alpha$. Following this discussion we will not be using this re-parameterization.

Examining this stability diagram, we see that as $A = \mu - \nu$ increases across the saddle node bifurcation two chimerical equilibria are born, in addition to the omnipresent equilibrium in which both populations are fully clustered. For small enough $\beta = \pi/2 - \alpha$ (falling in the region labelled "stable chimera") one of these chimera is stable, the other a saddle. From this stable chimera region, as $A = \mu - \nu$ increases the system goes through a supercritical Hopf bifurcation and a stable limit cycle is born around the previously stable chimera equilibrium. With A increasing further there is a homoclinic bifurcation, destroying the limit cycle and leaving one unstable and one saddle equilibrium chimera. It is of interest to note that trajectories on the limit cycle are known as "breathing" chimera, as the order parameter ρ of the partially dispersed population fluctuates regularly in time.

One note which will be of particular interest is that due to the intersection of the saddle node bifurcation with the A, β origin there is then no region of parameter space with $\nu \geq \mu > 0$ which admits chimera.

As mentioned above, due to symmetry considerations the parameter space $\mu < 0, \nu < 0$ must exhibit exactly the same behaviour as that described directly above, but with opposite stabilities, as the transformation $\mu \to -\mu$ and $\nu \to -\nu$ is equivalent to a reversal of time. Considering the transformation $\theta_i^\sigma \to \theta_i^\sigma + \pi$ for exactly one σ, we see from the

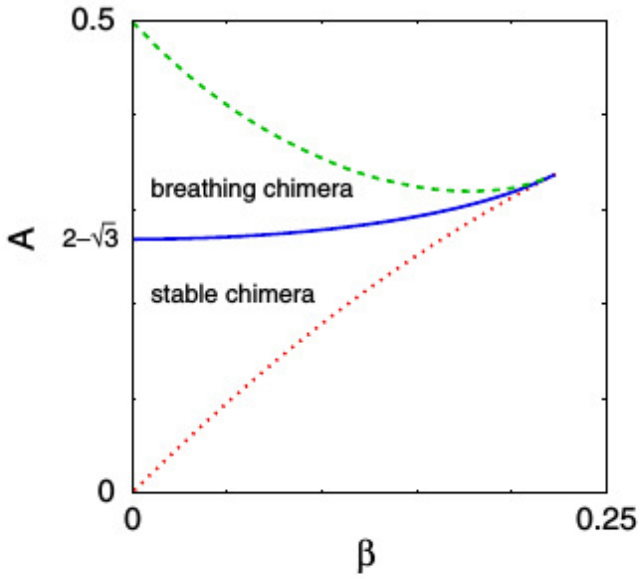

FIG. 4 (color online). Stability diagram for chimera states. Bifurcation curves: saddle-node (dotted line) and supercritical Hopf (solid line), both found analytically; homoclinic (dashed line), found numerically. All three curves intersect at a Takens-Bogdanov point $(\beta, A) = (\cos^{-1}\sqrt{\sqrt{13}/8 + 1/2}, \frac{3-\sqrt{2\sqrt{13}-5}}{3+\sqrt{2\sqrt{13}-5}}) = (0.2239, 0.3372)$.

Figure 1.2: Stability Diagram for Chimera. (Reprinted from [6])

governing system equations (1.13) that this is equivalent to the transformation $\nu \to -\nu$. Thus the regions of parameter space in which the inter and intra coupling coefficients have opposite sign are identical to (up to stability reversal) the regions so far examined. Therefore, without any loss of generality, we may continue to restrict our attention to the parameter space $0 \leq \alpha \leq \frac{\pi}{2}$ and both $\mu, \nu > 0$.

Examples of traditional chimera ($\rho_1 = 1$, $\rho_2 \neq 1$) are shown in figures 1.3 and 1.4, which contain sub-plots of: the time evolution of ρ_1, ρ_2, and ψ; the distribution of the population 2 at $t = 0$ and at the termination of the simulation plotted against the initial continuous PKD; a time series of the individual oscillator phase values for each sub-population. To generate figure 1.3 the system parameters $\alpha = 1.4708, \mu = .6, \nu = .4$

and initial conditions resulting in $\rho_1 = 1, \rho_2 = 0.7291$, and $\psi = -0.2094$ were used, which result in a stable chimera (both sub-populations have constant order parameter magnitude). Figure 1.4 displays a breathing chimera, in which the partially dispersed sub-population has variable order parameter magnitude. System parameters $\alpha = 1.4708, \mu = .64, \nu = .36$ (μ and ν different from previous simulation) and initial conditions resulting in $\rho_1 = 1, \rho_2 = 0.7291$, and $\psi = -0.2094$ (same as the previous simulation) were used for this simulation.

1.4 New Directions

Expanding on the definition of chimera, in which one sub-population is fully clustered ($\rho = 1$, phase- and frequency-locked) while the other is in a state of at least partial dispersal ($\rho \neq 1$), we will determine the conditions under which the above two-population version of the Kuramoto model (1.13) is able to persist in a "generalized" chimerical state, which we define to be a state in which both sub-populations are partially dispersed, and at least one of them has a constant order parameter magnitude.

Examining (1.18) we see immediately that both populations completely dispersed ($\rho_1 = \rho_2 = 0$) is an equilibrium state for this system. Also from (1.18), that if either population is completely dispersed ($\rho_\sigma = 0$) while the the other has non zero order parameter ($\rho_{\sigma'} \neq 0$) then $\dot{\rho}_\sigma > 0$ and we are immediately return to the quadrant of phase space $\rho_\sigma > 0, \rho_{\sigma'} > 0$. These observations, combined with the complete characterization of the case $\rho_\sigma = 1$ for at least one σ in [6] allow us to restrict our attention to the cases where $\rho_1, \rho_2 \in (0, 1)$.

Additionally, if $\nu = 0$ then the two sub-populations are non interacting, and the system has been reduced to two independent globally coupled Kuramoto models with phase lag, which has been completely analyzed in terms of its order parameter behaviour ((1.10) and (1.11)). Thus we may slightly further restrict parameter space, disallowing $\nu = 0$. While $\nu = 0$ represents a trivial reduction of the system, $\mu = 0$ results in the oscillators being coupled in a bipartite manner rather than the system having complete coupling, which constitutes an interesting (non-trivial) variation on the model. We will characterize the conditions for generalized chimera first with complete coupling ($\mu \neq 0$), and then

with bipartite coupling ($\mu = 0$). Note that no chimera (in the traditional sense) can exist with bipartite coupling, as $\mu = 0$ and $\nu > 0$ falls in the region of parameter space which does not admit chimerical solutions. We will accomplish this characterization entirely analytically. We will, however, also implement numerical routines to demonstrate the thus predicted behaviour, displaying the time evolution of order parameters as well as the motion of the individual oscillators. As a final note, from this point on we will entirely drop the explicit function notation indicating dependence on time, where thus far it has been sometimes included for clarity.

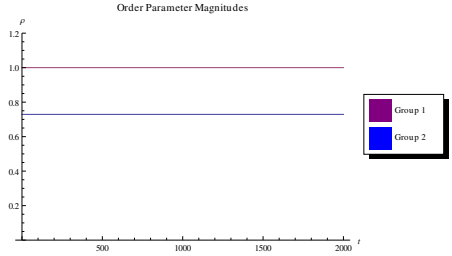

(a) The order parameter magnitudes ρ_1 and ρ_2 evolving in time.

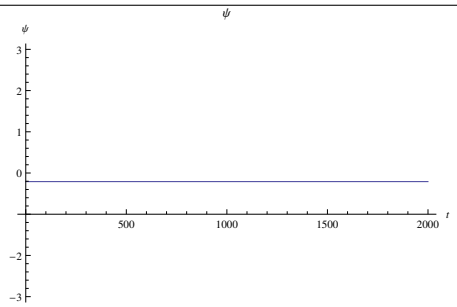

(b) The difference in order parameter arguments $(\psi = \phi_1 - \phi_2)$ evolving in time.

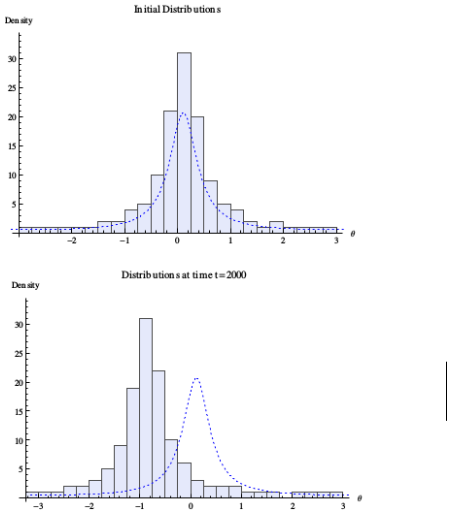

(c) Distribution of group 2 at times $t = 0$ and $t = 2000$. The dashed line is the initial continuous PKD and the bar graph is the distribution of θ values.

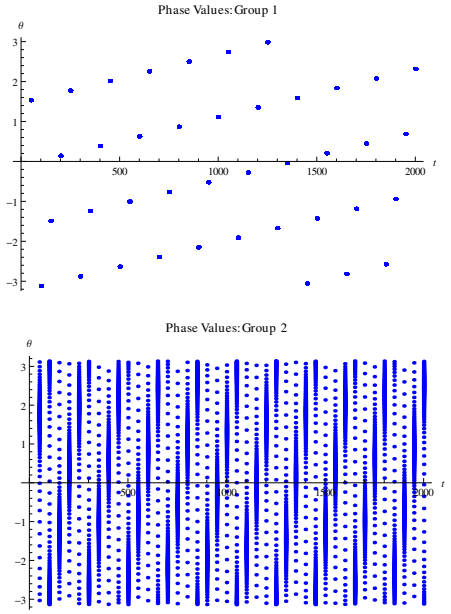

(d) Time series of the actual phase values, for groups 1 and 2, shown at times $t = 5, 10, 15, ...2000$.

Figure 1.3: Traditional Chimera: Stable Chimera

.

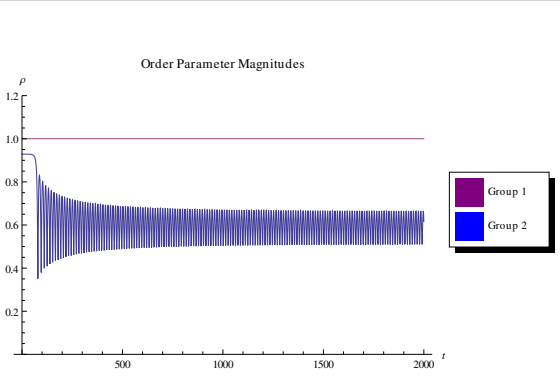

(a) The order parameter magnitudes ρ_1 and ρ_2 evolving in time.

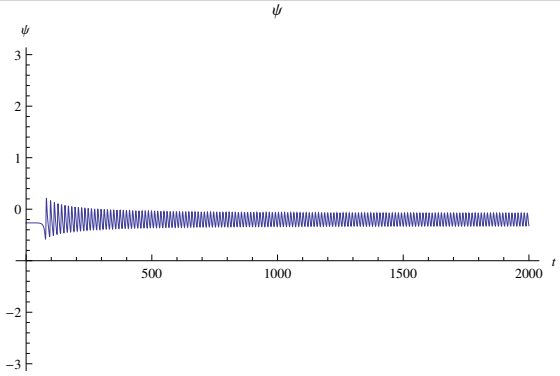

(b) The difference in order parameter arguments ($\psi = \phi_1 - \phi_2$) evolving in time.

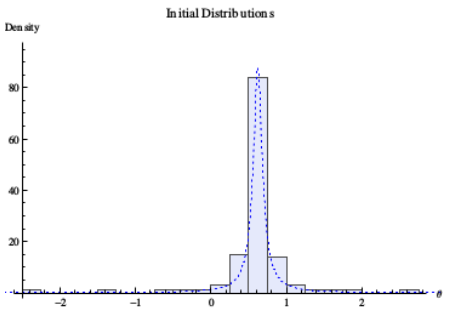

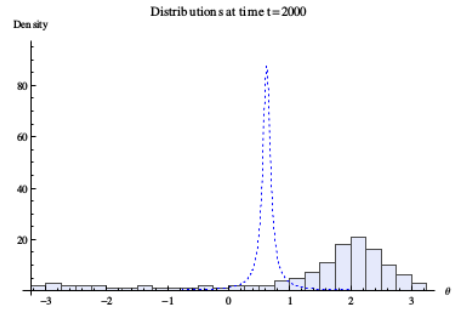

(c) Distribution of group 2 at times $t = 0$ and $t = 2000$. The dashed line is the initial continuous PKD and the bar graph is the distribution of θ values.

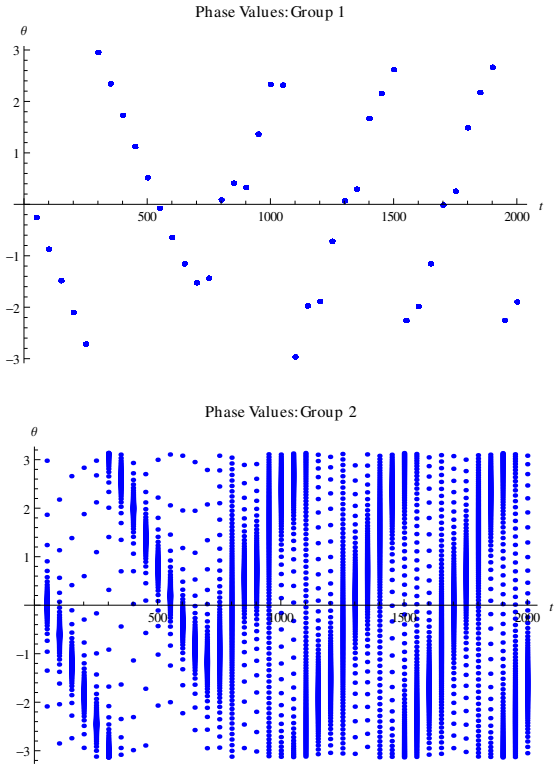

(d) Time series of the actual phase values, for groups 1 and 2, shown at times $t = 5, 10, 15, ...2000$.

Figure 1.4: Traditional Chimera: Breathing Chimera

.

Chapter 2

Analysis of the Model with Complete Coupling

In this chapter we will examine states in the phase space of the system (1.14),(1.15), with $\mu \neq 0$ which exist on the PKD manifold. That is, solutions of the system of two sub-populations of Kuramoto oscillators which are all coupled to each other (complete coupling), but with one constant coupling coefficient μ for intra-group coupling and another, ν, for inter-group coupling. Employing the transformation $\psi = \phi_1 - \phi_2$, the evolution equations for ρ_1, ρ_2 and ψ are (from 1.17)

$$\dot{\rho}_1(t) = \frac{1}{2}\left[1-\rho_1^2\right]\left[\mu\rho_1\cos(\alpha) + \nu\rho_2\cos(\psi+\alpha)\right] \tag{2.1}$$

$$\dot{\rho}_2(t) = \frac{1}{2}\left[1-\rho_2^2\right]\left[\mu\rho_2\cos(\alpha) + \nu\rho_1\cos(\psi-\alpha)\right] \tag{2.2}$$

$$\begin{aligned}\dot{\psi}(t) = &-\frac{1}{2}\left[1+\rho_1^2\right]\left[\mu\sin(\alpha) + \nu\frac{\rho_2}{\rho_1}\sin(\psi+\alpha)\right] \\ &+ \frac{1}{2}\left[1+\rho_2^2\right]\left[\mu\sin(\alpha) - \nu\frac{\rho_1}{\rho_2}\sin(\psi-\alpha)\right]\end{aligned} \tag{2.3}$$

Our interest is in generalized chimerical solutions, in which both sub-populations are partially clustered, with at least one population having constant order parameter magnitude. As discussed in section 1.4 we need not consider $\rho = 0, 1$ for either sub-population.

Theorem 2.1 *Generalized Chimera are trajectories through phase space in which one of two sub-populations has a constant order parameter magnitude while that of the other*

sub-population may vary. Traditional Chimera are those of the preceding states in which the sub-population with constant order parameter magnitude ρ_σ has $\rho_\sigma = 1$.
For the system (1.14),(1.15), with $\mu > 0, \nu > 0, 0 \leq \alpha \leq \frac{\pi}{2}$ and for points on the PKD manifold, generalized (non-traditional) chimera exist if and only if the system occupies one of the following equilibrium states:

- *Case One: $\alpha = \frac{\pi}{2}, \psi = 0,$ and $\rho_1\rho_2 = \frac{\nu}{\mu}$*
- *Case Two: $\alpha = \frac{\pi}{2}, \psi = 0, \pi,$ and $\rho_1 = \rho_2$*
- *Case Three: $\psi = \pi, \rho_1 = \rho_2,$ and $\nu = \mu$*

Note that this excludes the possibility of having one population which is constantly partially clustered while the clustering of the other sub-population varies in time.
We will prove this by first considering the case $\dot{\rho}_1 = \dot{\rho}_2 = 0$ in section 2.1, and then showing in section 2.2 that the general case $\dot{\rho}_1 = 0, \dot{\rho}_2 = \dot{\rho}_2(t)$ admits no further solutions. Having done so, we will complete this chapter by exhibiting these generalized chimera through numerical simulations in section 2.3.

2.1 Two Constant Order Parameter Magnitudes

Assuming that $\dot{\rho_1} = \dot{\rho_2} = 0$, $\rho_1, \rho_2 \in (1, 0)$, $\mu > 0, \nu > 0$ the $\dot{\rho_\sigma}$ equations of motion (2.1) and (2.2) reduce to

$$0 = \mu\rho_1 \cos(\alpha) + \nu\rho_2 \cos(\psi + \alpha) \tag{2.4}$$

$$0 = \mu\rho_2 \cos(\alpha) + \nu\rho_1 \cos(\psi - \alpha) \tag{2.5}$$

Multiplying the above two equations together results in

$$\begin{aligned} \mu^2 \cos^2(\alpha) &= \nu^2 \cos(\psi + \alpha)\cos(\psi - \alpha) \\ &= \nu^2 \frac{1}{2}\left[\cos(2\psi) + \cos(2\alpha)\right] \\ &= \nu^2 \frac{1}{2}\left[2\cos^2(\psi) - 1 + 2\cos^2(\alpha) - 1\right] \\ &= \nu^2\left[\cos^2(\psi) + \cos^2(\alpha) - 1\right] \\ \Leftrightarrow \cos^2(\psi) &= 1 - \cos^2(\alpha)\left[1 - \frac{\mu^2}{\nu^2}\right] \end{aligned} \tag{2.6}$$

Which requires $\dot{\psi} = 0$, since this specifies ψ in terms of constant system parameters. Since it must be that $\cos^2(\psi) \leq 1$ this restricts us further to the region $\nu \geq \mu > 0$. Since $\rho_1, \rho_2, \nu, \mu \neq 0$, from (2.4) and (2.5) we note that any one of $\cos(\alpha), \cos(\psi - \alpha)$, and $\cos(\psi + \alpha)$ is zero if and only if the others are as well, which is equivalent to $\psi = 0, \pi$ and $\alpha = \frac{\pi}{2}$. This case will be handled separately following this analysis. Assuming that this is not the case we may divide (2.4) by (2.5) to get

$$\begin{aligned} \frac{\rho_1}{\rho_2} &= \frac{\rho_2}{\rho_1}\frac{\cos(\psi+\alpha)}{\cos(\psi-\alpha)} \\ \Leftrightarrow \frac{\rho_1^2}{\rho_2^2} &= \frac{\cos(\psi+\alpha)}{\cos(\psi-\alpha)} \end{aligned} \tag{2.7}$$

Multiplying (2.3) by $2\rho_1/\rho_2$ we express the equation of motion for ψ becomes

$$\begin{aligned} 0 &= 2\frac{\rho_1}{\rho_2}\dot{\psi} \\ &= -\left[1+\rho_1^2\right]\left[\mu\frac{\rho_1}{\rho_2}\sin(\alpha) + \nu\sin(\psi+\alpha)\right] + \left[1+\rho_2^2\right]\left[\mu\frac{\rho_1}{\rho_2}\sin(\alpha) - \nu\frac{\rho_1^2}{\rho_2^2}\sin(\psi-\alpha)\right] \\ &= \mu\frac{\rho_1}{\rho_2}\sin(\alpha)\left[\rho_2^2-\rho_1^2\right] - \nu\rho_1^2\left[\sin(\psi+\alpha)+\sin(\psi-\alpha)\right] - \nu\left[\sin(\psi+\alpha) + \frac{\rho_1^2}{\rho_2^2}\sin(\psi-\alpha)\right] \\ 0 &= \mu\rho_1\rho_2\sin(\alpha)\left[1-\frac{\rho_1^2}{\rho_2^2}\right] - 2\nu\rho_1^2\sin(\psi)\cos(\alpha) - \nu\left[\sin(\psi+\alpha)+\frac{\rho_1^2}{\rho_2^2}\sin(\psi-\alpha)\right] \end{aligned}$$

Substituting $\rho_1^2/\rho_2^2 = \cos(\psi+\alpha)/\cos(\psi-\alpha)$ (2.7) and multiplying through by $\cos(\psi-\alpha)$ results in the constraint

$$\begin{aligned} 0 =& \mu\rho_1\rho_2\sin(\alpha)\left[\cos(\psi-\alpha)-\cos(\psi+\alpha)\right] - 2\nu\rho_1^2\sin(\psi)\cos(\alpha)\cos(\psi-\alpha) \\ &- \nu\left[\sin(\psi+\alpha)\cos(\psi-\alpha)+\cos(\psi+\alpha)\sin(\psi-\alpha)\right] \\ =& 2\mu\rho_1\rho_2\sin^2(\alpha)\sin(\psi) - 2\nu\rho_1^2\sin(\psi)\cos(\alpha)\cos(\psi-\alpha) - \nu\sin(2\psi) \end{aligned} \tag{2.8}$$

We can eliminate the $\cos(\psi-\alpha)$ term by rearranging and equating expressions (2.6) and (2.7)

$$\begin{aligned} \tfrac{\rho_1^2}{\rho_2^2} = \cos(\psi+\alpha)/\cos(\psi-\alpha) \quad &\Rightarrow \quad \tfrac{\rho_1^2}{\rho_2^2}\cos(\psi-\alpha) = \cos(\psi+\alpha) \\ \mu^2\cos^2(\alpha) = \nu^2\cos(\psi+\alpha)\cos(\psi-\alpha) \quad &\Rightarrow \quad \mu^2\cos^2(\alpha)/\left[\nu^2\cos(\psi-\alpha)\right] = \cos(\psi+\alpha) \\ &\Rightarrow \quad \tfrac{\rho_1^2}{\rho_2^2}\cos^2(\psi-\alpha) = \mu^2\cos^2(\alpha)/\nu^2 \\ &\Rightarrow \quad \mid\cos(\psi-\alpha)\mid = (\mu/\nu)(\rho_2/\rho_1)\mid\cos(\alpha)\mid \end{aligned}$$

Referencing (2.5) and since $\text{sgn}[\cos(\alpha)] = +1$ we see that $\text{sgn}\left[\cos(\psi - \alpha)\right] = -1$. Thus, substituting the above into (2.8) we get

$$\begin{aligned} 0 &= 2\mu\rho_1\rho_2 \sin^2(\alpha)\sin(\psi) + 2\mu\rho_1\rho_2 \cos^2(\alpha)\sin(\psi) - \nu\sin(2\psi) \\ &= 2\mu\rho_1\rho_2 \sin(\psi) - \nu\sin(2\psi) \\ &= 2\mu\rho_1\rho_2 \sin(\psi) - 2\nu\sin(\psi)\cos(\psi) \\ &\Rightarrow 0 = \mu\rho_1\rho_2 - \nu\cos(\psi) \\ &\Rightarrow \rho_1\rho_2 = \nu\cos(\psi)/\mu \end{aligned} \tag{2.9}$$

unless $\sin(\psi) = 0$, which will be considered at the end of this section as our second special case.

As $\rho_1\rho_2 < 1$, equation (2.9) requires that $\mid \cos(\psi) \mid < \mu/\nu$. Referring back to (2.6) and recalling that $\mu \leq \nu$ we see that

$$\begin{aligned} \frac{\mu^2}{\nu^2} &> \cos^2(\psi) \\ &= 1 - \cos^2(\alpha)\left[1 - \frac{\mu^2}{\nu^2}\right] \\ &\Rightarrow \cos^2(\alpha) > 1 \end{aligned}$$

Which is identically false. Thus the only region in which generalized chimerical behaviour could exist is in the so far excluded special cases: that $\sin(\psi) = 0$, or that $\psi = 0, \pi$ and $\alpha = \frac{\pi}{2}$. In both cases $\psi = 0, \pi$ and the ρ_σ equations of motion ((2.4) and (2.5)) become

$$\begin{aligned} 0 &= \cos(\alpha)\left[\mu\rho_1 + \nu\rho_2\cos(\psi)\right] \\ 0 &= \cos(\alpha)\left[\mu\rho_2 + \nu\rho_1\cos(\psi)\right] \end{aligned}$$

If $\cos(\alpha) \neq 0$ then by inspection we see that $\rho_1 = \rho_2$, that $\psi = \pi$, and that $\mu = \nu$. Substituting these conditions into the ψ equation of motion (2.3) results in the trivial tautology $0 = 0$. Thus the equilibria described by case 3 of theorem 2.1 exist.

If $\cos(\alpha) = 0$ then the ρ_σ equations of motion (2.1) and (2.2) are immediately satisfied, and the ψ equation of motion (2.3) reduces to

$$0 = \left[\rho_2^2 - \rho_1^2\right]\left[\mu\rho_1\rho_2 - \nu\cos(\psi)\right]$$

Thus $\rho_1 = \rho_2$ (Case 2, thm 2.1) or $\cos(\psi) = \mu\rho_1\rho_2/\nu \Rightarrow \psi = 0$ (since the RHS is positive and $\psi = 0, \pi$) and $\rho_1\rho_2 = \nu/\mu$ (Case 1, thm 2.1).

This completes the demonstration that the families of equilibria outlined in theorem 2.1 all exist. In the remainder of the chapter we will show that there are no generalized chimera in which either population has non-constant order parameter magnitude.

Due to the symmetry considerations discussed throughout the Introduction, the equilibria which exist throughout the remainder of non zero parameter space (one or both of μ and ν negative, α not restricted to $[0, \frac{\pi}{2}]$) are simply repetitions of the equilibria derived above. Thus our analysis extends to the entire (non zero for μ, ν) parameter space, and that generalized chimeras with both order parameter magnitudes constant in time occur, for this type of model and on the PKD manifold, exactly and only for the conditions enumerated in Theorem 2.1.

2.2 Exactly One Non-Constant Order Parameter Magnitude

Assuming now that $\dot{\rho_2} \neq 0$, and maintaining $\dot{\rho_1} = 0$ with $\rho_1, \rho_2 \in (1, 0), \mu > 0, \nu > 0$, and $0 \leq \alpha \leq \frac{\pi}{2}$ the system equations (2.1)-(2.3) reduce to

$$0 = \mu\rho_1 \cos(\alpha) + \nu\rho_2 \cos(\psi + \alpha) \tag{2.10}$$

$$\dot{\rho_2} = \frac{1 - \rho_2^2}{2} \left[\mu\rho_2 \cos(\alpha) + \nu\rho_1 \cos(\psi - \alpha)\right] \tag{2.11}$$

$$\dot{\psi} = -\frac{1 + \rho_1^2}{2} \left[\mu \sin(\alpha) + \nu\frac{\rho_2}{\rho 1} \sin(\psi + \alpha)\right] + \frac{1 + \rho_2^2}{2} \left[\mu \sin(\alpha) - \nu\frac{\rho_1}{\rho 2} \sin(\psi - \alpha)\right] \tag{2.12}$$

Equation (2.10) provides a restriction on the relative values of ρ_2 and ψ as well as their time derivatives. Specifically,

$$\rho_2 = -\frac{\mu\rho_1 \cos(\alpha)}{\nu \cos(\psi + \alpha)} \tag{2.13}$$

$$\dot{\rho_2} \cos(\psi + \alpha) = \rho_2 \sin(\psi + \alpha)\dot{\psi} \tag{2.14}$$

This allows us to use (2.13) to eliminate ρ_2 and to express $\dot{\psi}$ in two ways: once from the evolution equation for ψ (2.12) and once using (2.14) and substituting in the evolution

equation for ρ_2, (2.11). This results in two expressions for $\dot{\psi}$ in terms of one phase variable (ψ) and three constants - the ratio $\lambda := \mu/\nu, \alpha$, and ρ_1, where we have introduced λ only to simplify the following long expressions.

We now substitute (2.11) and (2.13) into (2.14), solve for $\dot{\psi}$, and expanding the right hand side (using Mathematica) into a sum of exponentials in ψ. We will expand our other expression for $\dot{\psi}$ as well, and as we wish to compare them, and they both contain denominator terms, we will pre-emptively gain a common denominator. The numerator of the equation (2.14) is then,

$$\begin{aligned} Numerator[\dot{\psi}] \quad &= \Big[- e^{-i3\alpha}\Big]e^{-5\psi} + \Big[(\lambda^2-1)e^{-i5\alpha} + (\lambda^2\rho_1^2 + 2\lambda^2)e^{-i3\alpha} + \\ &+(2\lambda^2\rho_1^2 + \lambda^2 - 4)e^{-i\alpha} + (\lambda^4\rho_1^2)e^{i\alpha}\Big]e^{-i3\psi} + \Big[(-\lambda^4\rho_1^2 + \lambda^2\rho_1^2)e^{-i5\alpha} + \\ &+(-4\lambda^4\rho_1^2 + 2\lambda^2\rho_1^2 + 3\lambda^2 - 4)e^{-i3\alpha} + (-6\lambda^4\rho_1^2 + 3\lambda^2\rho_1^2 + \lambda^2)e^{-i\alpha} + \\ &+(-4\lambda^4\rho_1^2 + 2\lambda^2\rho_1^2 + 3\lambda^2 - 6)e^{i\alpha} + (-\lambda^4\rho_1^2 + 2\lambda^2\rho_1^2)e^{i3\alpha}\Big]e^{-i\psi} + \\ &+[C.C.] \end{aligned} \tag{2.15}$$

Where $+[C.C.]$ means to add on the complex conjugate of everything appearing above. Expanding the numerator of our original expression for $\dot{\psi}$ gives

$$\begin{aligned} Numerator[\dot{\psi}] \quad &= \Big[- e^{-i3\alpha}\Big]e^{-5\psi} + \Big[(-\lambda^2+1)e^{-i5\alpha} + (\lambda^2\rho_1^2 + 2\lambda^2)e^{-i3\alpha} + \\ &+(3\lambda^2 - 2)e^{-i\alpha} + (-\lambda^2\rho_1^2)e^{i\alpha}\Big]e^{-i3\psi} + \Big[(-\lambda^4\rho_1^2 + \lambda^2\rho_1^2)e^{-i5\alpha} + \\ &+(-2\lambda^4\rho_1^2 + 4\lambda^2\rho_1^2 + \lambda^2 + 2)e^{-i3\alpha} + (3\lambda^2\rho_1^2 + 2\lambda^2)e^{-i\alpha} + \\ &+(2\lambda^4\rho_1^2 + \lambda^2)e^{i\alpha} + (\lambda^4\rho_1^2)\Big]e^{-i\psi} + \\ &+[C.C.] \end{aligned} \tag{2.16}$$

The (common) denominator is the product $2\lambda\cos(\alpha)\cos^2(\psi+\alpha)\sin(\psi+\alpha)$. As discussed previously, any of these terms being zero requires all the others to be as well, and reduces the resulting solution to an equilibrium. We may thus disregard the denominator, as we are interested in conditions under which the difference of these two expressions is zero. Taking the difference (disregarding the denominator) and setting equal to zero gives the

condition

$$\begin{aligned} 0 \quad &= \Big[0\Big]e^{-i5\psi} + \Big[(-2\lambda^2+2)e^{-i5\alpha} + (0)e^{-i3\alpha} + \\ &+(-2\lambda^2\rho_1^2 + 2\lambda^2 + 2)e^{-i\alpha} + (-2\lambda^2\rho_1^2)e^{i\alpha}\Big]e^{-i3\psi} + \\ &+\Big[(0)e^{-i5\alpha} + (2\lambda^4\rho_1^2 + 2\lambda^2\rho_1^2 - 2\lambda^2 + 6)e^{-i3\alpha} + \\ &+(6\lambda^4\rho_1^2 - 4\lambda^2)e^{-i\alpha} + (6\lambda^4\rho_1^2 - 4\lambda^2\rho_1^2 - 2\lambda^2 + 6)e^{i\alpha} + \\ &+(2\lambda^4\rho_1^2 - 2\lambda^2\rho_1^2)e^{i3\alpha}\Big]e^{-i\psi} + [C.C.] \end{aligned} \tag{2.17}$$

Since each coefficient is not identically zero these are independent descriptions of $\dot{\psi}$, and create form a restriction on the system behaviour.

While the coefficients are not identically zero, there may yet be particular points in parameter space for which they are. To find these, first note that as the coefficient of $e^{in\psi}$ is the complex conjugate of the coefficient of $e^{-in\psi}$ such pairs form redundant constraints, and so we need only examine, for instance, the coefficients of $e^{-i5\psi}$, $e^{-i3\psi}$, and $e^{-i\psi}$. The coefficient of $e^{-i5\psi}$ is identically zero, so this does not constrain the parameters. Setting the coefficient of $e^{-i3\psi}$ to zero results in two equalities, for the real and imaginary parts. The imaginary terms give the condition

$$\lambda^2 := \frac{\mu^2}{\nu^2} = \frac{\sin(5\alpha) + \sin(\alpha)}{\sin(5\alpha) - \sin(\alpha)}$$

While the real part can be re-written to give ρ_1^2 as a function of α and λ^2. Substituting in the above expression for λ^2 and simplifying gives,

$$\rho_1^2 = \frac{2}{1 + 2\cos(\alpha)}$$

The imaginary part of the equality derived from the $e^{-i\psi}$ term gives a second expression for ρ_1^2,

$$\rho_1^2 = \frac{1 - 2\cos(2\alpha)}{2 + 2\cos(2\alpha)}$$

Equating these two expressions for ρ_1^2 requires

$$0 \quad = 3 + 6\cos(2\alpha) + 2\cos(3\alpha) \tag{2.18}$$

This equality holds for only one value of $\alpha \in [0, \pi/2]$, at $\alpha \approx .888082$. Furthermore, the right hand side of (2.18) decreases continuously on the interval $.8 \leq \alpha \leq .9$, is positive

at $\alpha = 0.8$ and negative at $\alpha = 0.9$. Thus the root certainly lies somewhere in between. The one remaining independent condition on the parameters is the real part of the equation resulting from setting the coefficient of $e^{-i\psi}$ to zero. Numerically evaluating ρ_1^2 and λ^2 across $\alpha \in [0.8, 0.9]$ and substituting these values into this equation results in a continuous monotonic curve decreasing from approximately -1.5536 on the left side of the α interval to approximately -2.1095 on the right side of the interval. Since the left hand side of this constraining equality is zero, we may conclude that there are in fact no points in our parameter space at which these coefficients are zero. There are therefore no values of α for which these two expressions for $\dot{\psi}$ can be made to equate, which contradicts the assumptions leading to them - that is, there are no Generalized Chimerical solutions in which one order parameter magnitude is constant and less than one while the other fluctuates.

Having now shown that no additional chimera exist besides those found in section 2.1, this completes the proof of Theorem 2.1.

2.3 Numerical Simulations

According to Theorem 2.1, for an infinite population of oscillators distributed along a PKD we should observe generalized chimera in which the order parameter magnitudes of both sub-populations are constant and less than one iff one of the following holds:

- Case 1: $\alpha = \frac{\pi}{2}, \psi = 0$, and $\rho_1\rho_2 = \nu/\mu$
- Case 2: $\alpha = \frac{\pi}{2}, \psi = 0, \pi$, and $\rho_1 = \rho_2$
- Case 3: $\psi = \pi, \mu = \nu$, and $\rho_1 = \rho_2$

Here we present the results of numerical simulations of representative finite size versions of these cases. Throughout we will use population sizes $N_1 = N_2 = 128$, and the simulations are as follows:

Figure 2.1: Case 1 (thm 2.1), in which μ and ν are not constrained to be equal, but $\alpha = \frac{\pi}{2}, \psi = 0$, and $\rho_1\rho_2 = \nu/\mu$. We use $\mu = \frac{4}{7}, \nu = \frac{3}{7}$ and $\rho_1 = 15/16, \rho_2 = 4/5$.

Figure 2.2: Case 2 (thm 2.1), in which μ and ν are not constrained to be equal, but

$\alpha = \frac{\pi}{2}, \psi = 0, \pi$, and $\rho_1 = \rho_2$. We use $\mu = \frac{4}{7}, \nu = \frac{3}{7}, \rho_1 = \rho_2 = .75$, and $\psi = \pi$.
Figure 2.3: Similar to the second simulation (Case 2, thm 2.1), however this time we use $\psi = 0$.
Figure 2.4: Case 3 (thm 2.1), in which α is not constrained to be $\frac{\pi}{2}$, but $\psi = \pi, \mu = \nu$, and $\rho_1 = \rho_2$. We use $\alpha = \frac{4\pi}{9}$ and $\rho_1 = \rho_2 = .75$.

In each of these figures we see in subplots (a) that the order parameter magnitudes ρ_1 and ρ_2 are less than unity as required, and both constant as predicted. Also, in subplots (b) that ψ is constant as predicted. In subplots (c) we see that the distribution of oscillators in each sub-population retains the general shape of its original distribution along the chosen PKD, though in general (figures 2.2-2.1) the populations are in motion, and so the histograms are out of phase with the initial PKD. In subplots (c) we see the motion of the individual oscillators, affording insight into the machination of these chimera. Note only one population is visible in figure 2.2 (a) and in 2.3 in (a), (b), and (c): in 2.2 it is because the two have exactly equal order parameter magnitudes, and in 2.3 this is due to the two populations being identically distributed and exactly coincident.

Case 3, in which α is not constrained to be $\frac{\pi}{2}$, but $\psi = \pi, \mu = \nu$, and $\rho_1 = \rho_2$ and displayed in figure 2.4 is unique among these outcomes in that it is a very unstable equilibrium, decaying by time $t = 120$. This is likely do to the instability of the equilibrium itself and not a finite size effect as it is the only solution which exhibits such an instability. It is also unique in that while it persists the sub-populations are each stationary on $[0, 2\pi)$.
In conclusion, these simulations suggest that the behaviours predicted in Theorem 2.1 for infinite populations do manifest in systems with finite population sizes.

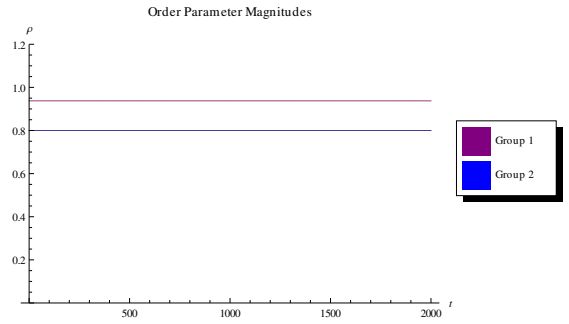

(a) The order parameter magnitudes ρ_1 and ρ_2 evolving in time.

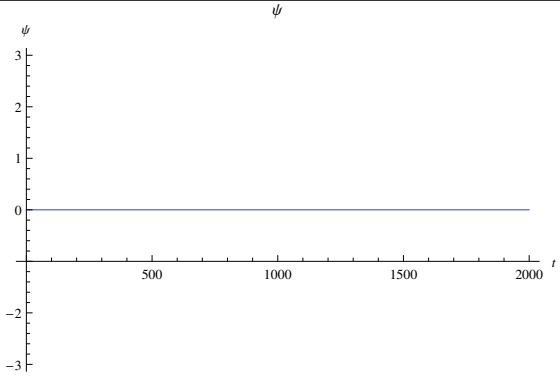

(b) The difference in order parameter arguments ($\psi = \phi_1 - \phi_2$) evolving in time.

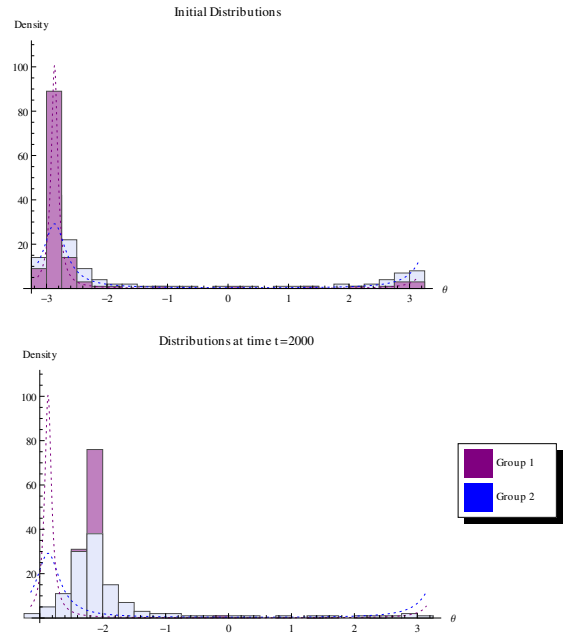

(c) Oscillator distributions at times $t = 0$ and $t = 2000$. The dashed lines are the initial continuous PKDs for each group, the bar graphs are the distributions of θ values.

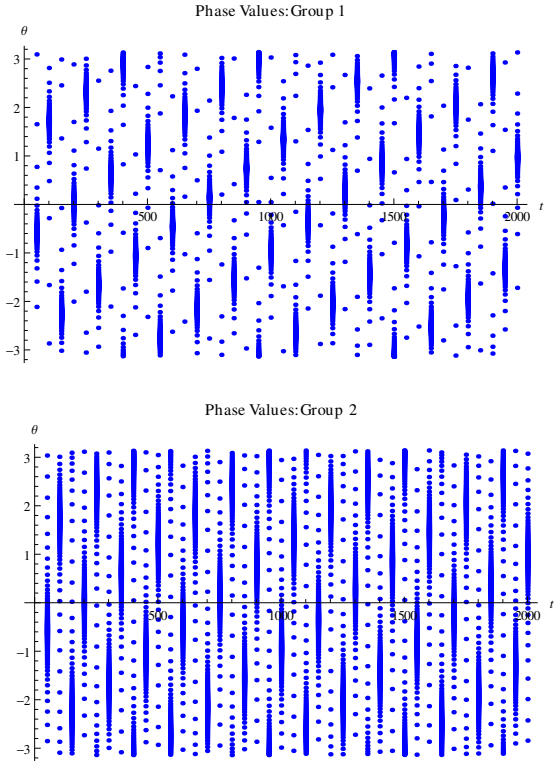

(d) Time series of the actual phase values, for groups 1 and 2, shown at times $t = 5, 10, 15, ...2000$.

Figure 2.1: Case 1 - Chimera with $\psi = 0, \alpha = \frac{\pi}{2}, \mu = \frac{4}{7}, \nu = \frac{3}{7}, \rho_1 = \frac{15}{16}$, and $\rho_2 = \frac{4}{5}$

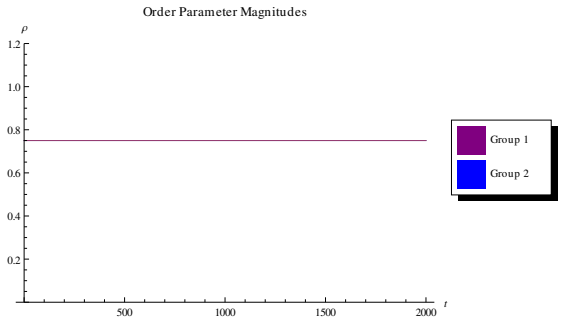

(a) The order parameter magnitudes ρ_1 and ρ_2 evolving in time. (ρ_1 and ρ_2 coincident here)

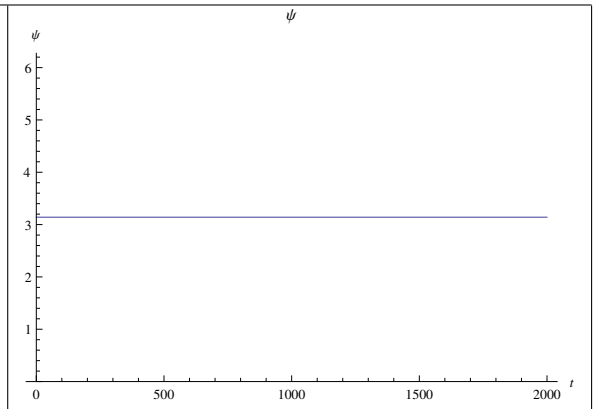

(b) The difference in order parameter arguments ($\psi = \phi_1 - \phi_2$) evolving in time.

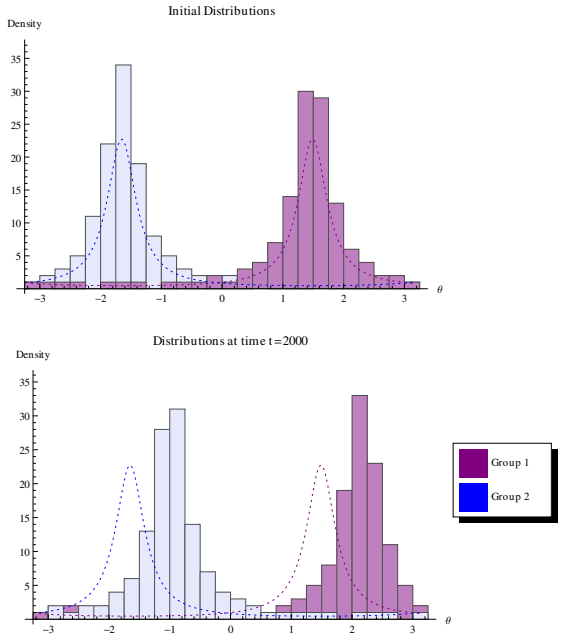

(c) Oscillator distributions at times $t = 0$ and $t = 2000$. The dashed lines are the initial continuous PKDs for each group, the bar graphs are the distributions of θ values.

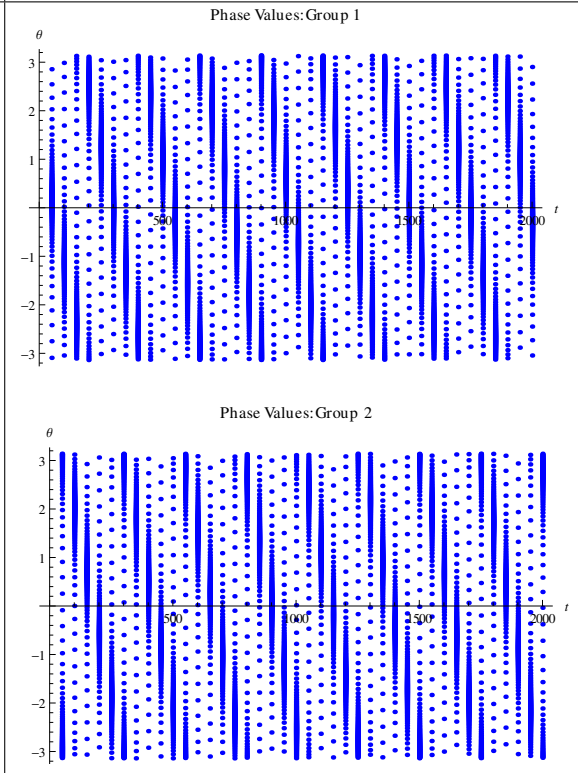

(d) Time series of the actual phase values, for groups 1 and 2, shown at times $t = 5, 10, 15, ...2000$.

Figure 2.2: Case 2 with $\psi = \pi$ - Chimera with $\alpha = \frac{\pi}{2}, \mu = \frac{4}{7}, \nu = \frac{3}{7}$, and $\rho_1 = \rho_2 = \frac{3}{4}$

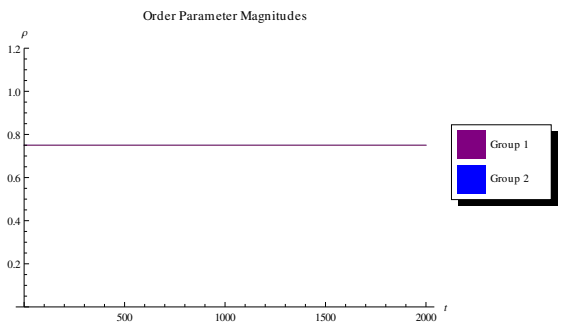

(a) The order parameter magnitudes ρ_1 and ρ_2 evolving in time. (ρ_1 and ρ_2 coincident here)

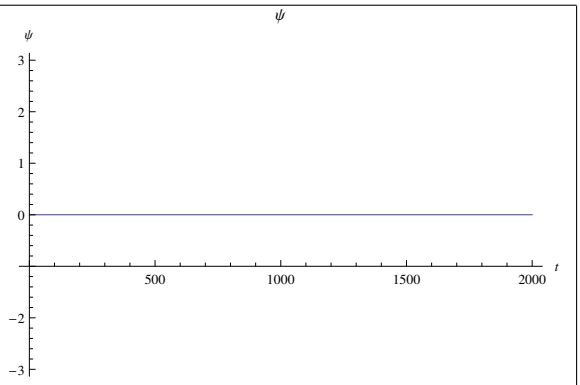

(b) The difference in order parameter arguments ($\psi = \phi_1 - \phi_2$) evolving in time.

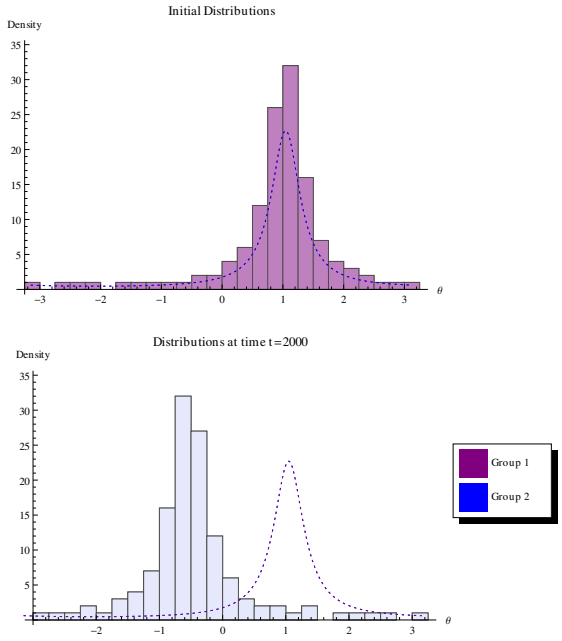

(c) Oscillator distributions at times $t = 0$ and $t = 2000$. The dashed lines are the initial continuous PKDs for each group, the bar graphs are the distributions of θ values.

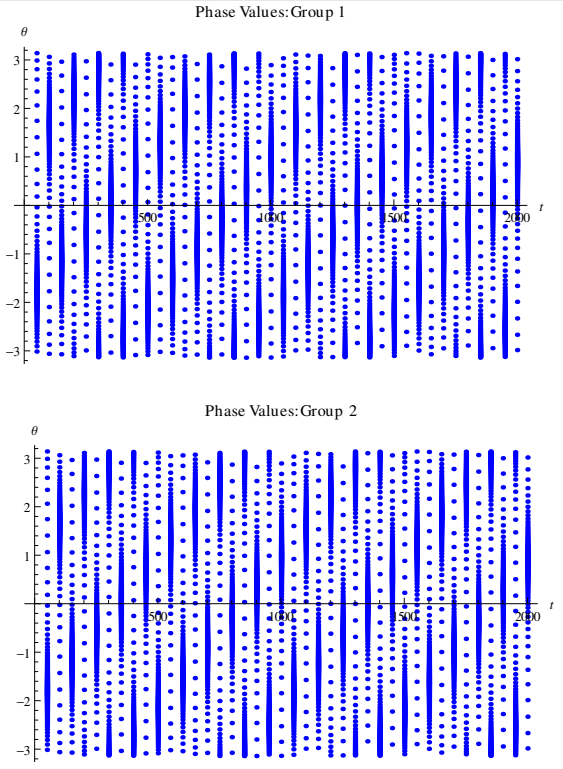

(d) Time series of the actual phase values, for groups 1 and 2, shown at times $t = 5, 10, 15, ...2000$.

Figure 2.3: Case 2 with $\psi = 0$ - Chimera with $\alpha = \frac{\pi}{2}, \mu = \frac{4}{7}, \nu = \frac{3}{7}$, and $\rho_1 = \rho_2 = \frac{3}{4}$

.

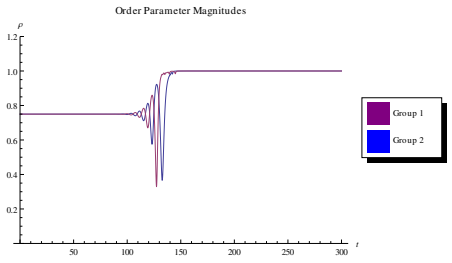

(a) The order parameter magnitudes ρ_1 and ρ_2 evolving in time.

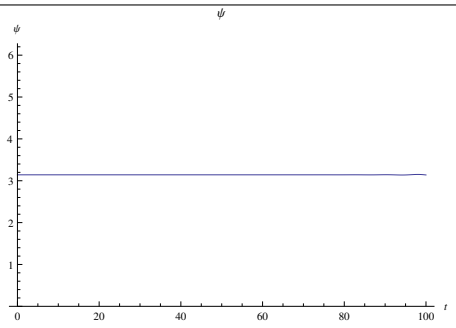

(b) The difference in order parameter arguments $(\psi = \phi_1 - \phi_2)$ evolving in time.

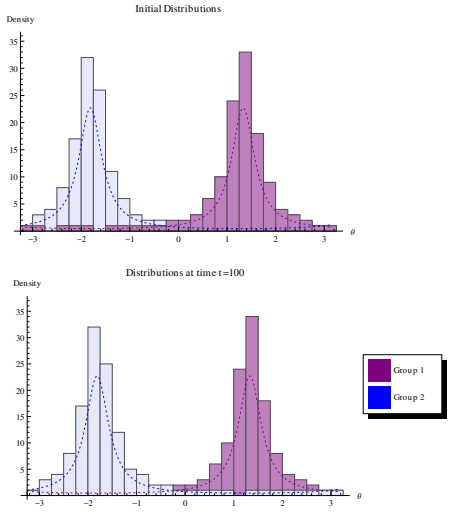

(c) Oscillator distributions at times $t = 0$ and $t = 100$. The dashed lines are the initial continuous PKDs for each group, the bar graphs are the distributions of θ values.

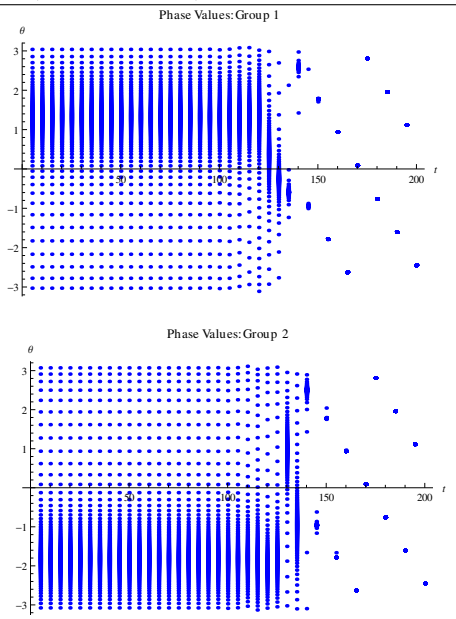

(d) Time series of the actual phase values, for groups 1 and 2, shown at times $t = 5, 10, 15, ...200$.

Figure 2.4: Case 3 - Chimera with $\psi = \pi, \alpha = \frac{4\pi}{9}, \mu = \nu = \frac{1}{2}$, and $\rho_1 = \rho_2 = \frac{3}{4}$

.

Chapter 3

Analysis of the Model with Bipartite Coupling

In this chapter we examine the limiting case $\mu = 0$ of the model (1.17), resulting in a system with bipartite coupling. Each oscillator in sub-population 1 is coupled to each oscillator in sub-population 2, however there is no intra-group coupling. We are still restricting our attention to points of phase space which lie on the PKD manifold, and are searching for generalized chimerical behaviour. As before, it is unnecessary to consider the points which result in either population having order parameter magnitude $\rho = 0$ or 1.

Theorem 3.1 *Generalized Chimera are trajectories through phase space in which one of two sub-populations has a constant order parameter magnitude while that of the other sub-population may vary. Traditional Chimera are those of the preceding states in which the sub-population with constant order parameter magnitude ρ_σ has $\rho_\sigma = 1$.*
For the system (1.14),(1.15), with $\mu = 0, \nu > 0, 0 \leq \alpha \leq \frac{\pi}{2}$ and for points on the PKD manifold, generalized chimera exist if and only if $\alpha = \frac{\pi}{2}, \psi = 0, \pi$, and $\rho_1 = \rho_2$.

3.1 Proof of Theorem 3.1

With $\mu = 0$ the evolution equations for the order parameters ρ_1, ρ_2, and ψ become (from (2.1) - (2.3))

$$\begin{aligned}
\dot{\rho_1} &= \frac{1}{2}\left[1-\rho_1^2\right]\nu\rho_2\cos(\psi+\alpha) \\
\dot{\rho_2} &= \frac{1}{2}\left[1-\rho_2^2\right]\nu\rho_1\cos(\psi-\alpha) \\
\dot{\psi} &= -\frac{1}{2}\left[1+\rho_1^2\right]\nu\frac{\rho_2}{\rho_1}\sin(\psi+\alpha) - \frac{1}{2}\left[1+\rho_2^2\right]\nu\frac{\rho_1}{\rho_2}\sin(\psi-\alpha)
\end{aligned}$$

and our assumptions are that $\dot{\rho}_1 = 0, \nu > 0$, and $0 \leq \alpha \leq \frac{\pi}{2}$. First we note that each term in the above equations contains a factor of $(1/2)\nu$, which therefore may be scaled out. Under these assumptions, and rescaling time to eliminate the factor of $\frac{1}{2}\nu$, these evolution equations become

$$0 = \left[1-\rho_1^2\right]\rho_2\cos(\psi+\alpha) \tag{3.1}$$

$$\dot{\rho_2} = \left[1-\rho_2^2\right]\rho_1\cos(\psi-\alpha) \tag{3.2}$$

$$\dot{\psi} = -\left[1+\rho_1^2\right]\frac{\rho_2}{\rho_1}\sin(\psi+\alpha) - \left[1+\rho_2^2\right]\frac{\rho_1}{\rho_2}\sin(\psi-\alpha) \tag{3.3}$$

As we do not allow $\rho = 0, 1$ for either population, equation (3.1) must be satisfied via the restriction $\cos(\psi+\alpha) = 0$, which immediately leads to $\dot{\psi} = 0$ and $\sin(\psi+\alpha) = \pm 1$. Multiplying through by $\mp\rho_1\rho_2$ the evolution equation for ψ (3.3) then reads

$$\begin{aligned}
0 &= \left[1+\rho_1^2\right]\rho_2^2 \pm \left[1+\rho_2^2\right]\rho_1^2\sin(\psi-\alpha) \\
&\Rightarrow \rho_2^2 = \frac{\mp\rho_1^2\sin(\psi-\alpha)}{1+\rho_1^2\left[1\pm\sin(\psi-\alpha)\right]} \\
&\Rightarrow \dot{\rho_2} = 0
\end{aligned}$$

Which conclusion regarding $\dot{\rho}_2$ follows because, by assumption $\rho_2 \neq 0, \dot{\rho}_1 = 0$; as a parameter $\dot{\alpha} = 0$, and by previous implication $\dot{\psi} = 0$. ρ_2 is then determined by constants, and so itself must be constant. Then, from the evolution equation for ρ_2 (3.2)

$$0 = \left[1-\rho_2^2\right]\rho_1\cos(\psi-\alpha)$$

Which requires $\cos(\psi - \alpha) = 0$. As ψ and α are already restricted by $\cos(\psi + \alpha) = 0$ it must be that $\psi = 0, \pi$ and $\alpha = \frac{\pi}{2}$. The evolution equation for ψ (3.3) then becomes

$$\begin{aligned} 0 &= \left[1 + \rho_1^2\right] \rho_2^2 - \left[1 + \rho_2^2\right] \rho_1^2 \\ &= \rho_1^2 \rho_2^2 \left[1 - 1\right] + \left[\rho_2^2 - \rho_1^2\right] \\ &\Rightarrow \rho_1 = \rho_2 \end{aligned}$$

Thus, generalized chimera exist on the PKD manifold for this model only under the condition $\psi = 0, \pi$ and $\alpha = \frac{\pi}{2}$ as well as requiring that $\rho_1 = \rho_2$, proving Theorem 3.1

3.2 Numerical Simulations

According to Theorem 3.1, for an infinite population of oscillators distributed along a PKD and with $\alpha = \frac{\pi}{2}$ and $\psi = \pi$ we should observe a generalized chimera in which the order parameter magnitudes of both sub-populations are constant and less than one iff $\rho_1 = \rho_2$. Here we present the results of a simulation of a representative finite size version of this system with population sizes $N_1 = N_2 = 128$ and $\rho_1 = \rho_2 = .8$. The results of the simulation are pictured in figure 3.1.

In 3.1 subfigure (a) each of the sub-populations has exactly the same order parameter magnitude, $\rho_1 = \rho_2 = .8$, and we see that they do remain constant in time, as does the difference $\psi = \phi_1 - \phi_2$ (subfigure (b)).

In subfigure (c) we see each oscillator sub-population approximately distributed according to the desired PKD at time $t = 0$ (at top), and then a comparison of the actual distribution and the PKD at a later time (at bottom). The actual distribution is out of phase with the initial generating PKD as the oscillator sub-populations are in motion, however we see that they maintain the general shape of their distribution, as we would expect.

In subfigure (d) is pictured a time series of the phase variables of sub-populations 1 and 2 (top and bottom, respectively), in which not only is the constant $\psi = \pi$ behaviour observable, but we also see the motion of the peak of the distribution of each group.

In conclusion, this simulation with finite population sizes $N_1 = N_2 = 128$ does exhibit the behaviour predicted in Theorem 3.1 for infinite populations.

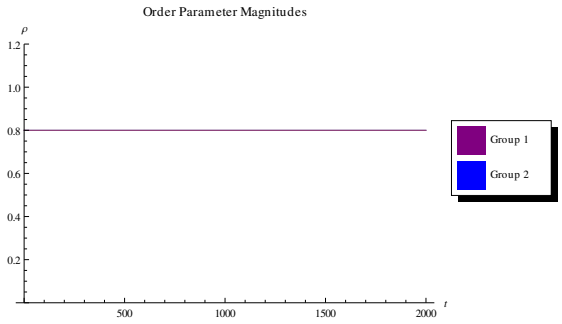

(a) The order parameter magnitudes ρ_1 and ρ_2 evolving in time. (ρ_1 and ρ_2 coincident here)

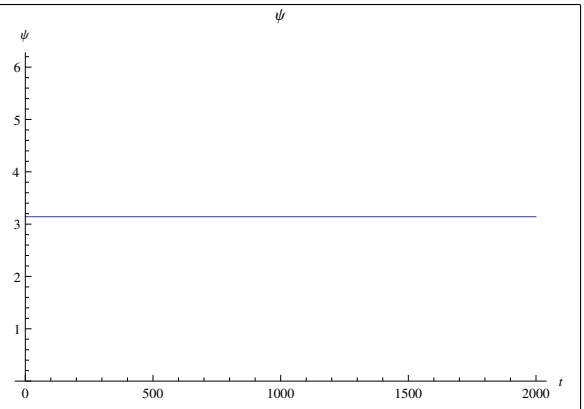

(b) The difference in order parameter arguments ($\psi = \phi_1 - \phi_2$) evolving in time.

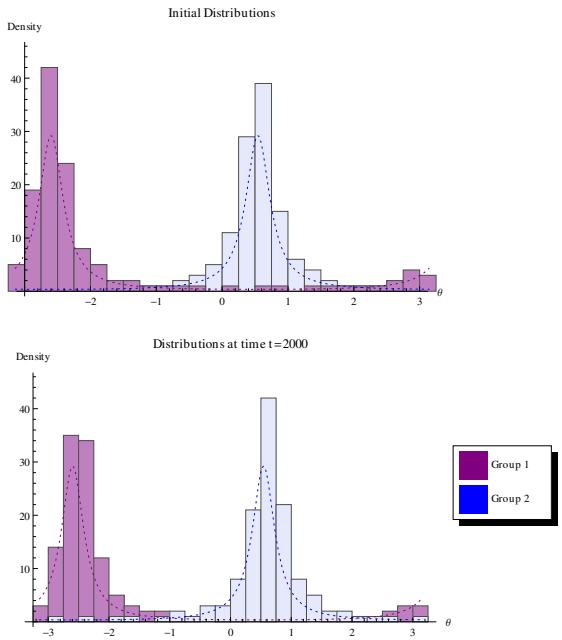

(c) Oscillator distributions at times $t = 0$ and $t = 2000$. The dashed lines are the initial continuous PKDs for each group, the bar graphs are the distributions of θ values.

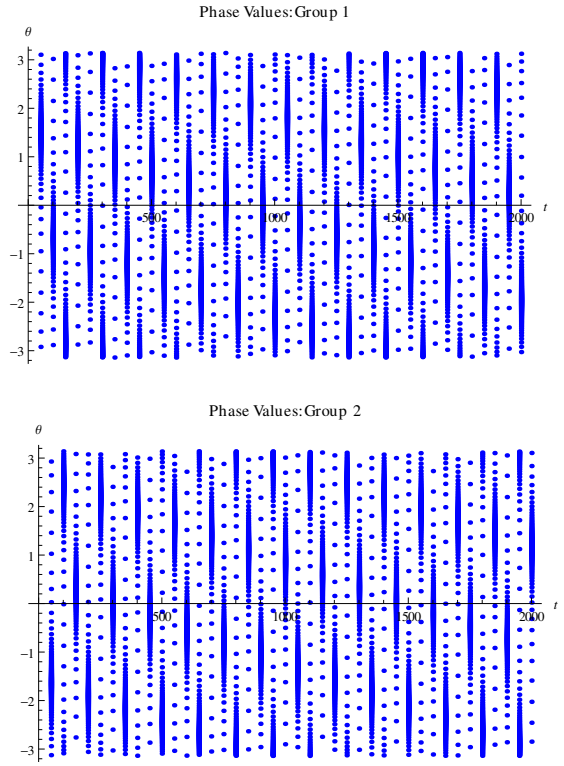

(d) Time series of the actual phase values, for groups 1 and 2, shown at times $t = 5, 10, 15, ...2000$.

Figure 3.1: Bipartite Chimera with $\alpha = \frac{\pi}{2}, \psi = \pi$, and $\rho_1 = \rho_2 = .8$

.

Chapter 4

Conclusions

We have examined a variation of the Kuramoto model in which the oscillators have identical natural frequencies, there is a common, constant phase lag, and the population of oscillators is divided into two groups with one constant coupling coefficient governing intra-group coupling and another for inter-group coupling. Further, we have dealt with two cases - a two-population model with complete coupling and a two-population model with bipartite coupling. In both cases we categorized the conditions under which the system exhibits what we have termed generalized chimerical behaviour, in which the two sub-populations both have non zero, non unity order parameter magnitudes, and at least one of which is constant in time. Specifically we have been interested in generalized chimera that are not traditional chimera - that is, our interest has been in the generalized chimera in which neither population is fully clustered, as the examination of traditional chimera for this model had been previously done.

We have found that generalized chimera (again, other than the traditionally termed chimera analyzed in [6]) only occur under very specific conditions, and as equilibrium solutions in 3-D phase space. Models with both complete and bipartite coupling admit chimerical equilibria when $\alpha = \frac{\pi}{2}, \psi = 0, \pi$, and $\rho_1 = \rho_2$. This is the full extent of the chimerical solutions with bipartite coupling, while complete coupling also exhibits chimera when (and only when, in addition to the above)

- $\alpha = \frac{\pi}{2}, \psi = 0$, and $\rho_1 \rho_2 = \frac{\nu}{\mu}$
- $\psi = \pi, \rho_1 = \rho_2$, and $\nu = \mu$

Note in this last case that $\mu = \nu$ - that is, the two populations of oscillators are acting on themselves and on each other equally.

Our numerical simulations demonstrate the existence of these chimera, as well as showing that they are reasonably persistent for finite sized populations of oscillators.

Thus expanding on the results of [6] we have contributed to the the problem of characterizing generalized chimera in the subset of phase space defined by the manifold of pairs of PKDs for the two-population Kuramoto model with phase lag.

References

[1] Yoshiki Kuramoto. *Self-entrainment of a population of coupled non-linear oscillators.* International Symposium on Mathematical Problems in Theoretical Physics, Lecture Notes in Physics, pages 420-422. Springer-Verlag Berlin, 1975.

[2] Edward Ott and Thomas Antonsen. *Low dimensional behaviour of large systems of globally coupled oscillators.* Chaos, 18:037113, 2008. doi:10.1063/1.2930766

[3] Edward Ott and Thomas Antonsen. *Long time evolution of phase oscillator systems.* Chaos, 19(2):023117, 2009. doi:10.1063/1.3136851.

[4] Edward Ott, Brian Hunt, and Thomas Antonsen. Comment on *Long time evolution of phase oscillator systems* [Chaos 19, 023117 (2009)]. Chaos, 21(2):025112, 2011. doi:10.1063/1.3574931.

[5] Yoshiki Kuramoto and Dorjsuren Battogtokh. *Coexistence of coherence and incoherence in nonlocally coupled phase oscillators.* Nonlinear Phenom. Complex Syst., 5(4):380-385, 2002.

[6] Daniel Abrams, Rennie Mirollo, Steven Strogatz, and Daniel Wiley. *Solvable model for chimera states of coupled oscillators.* Phys. Rev. Lett., 101:084103, 2008. doi:10.1103/PhysRevLett.101.084103.

[7] Steven Strogatz. *From Kuramoto to Crawford: Exploring the onset of synchronization in populations of coupled oscillators.* Physica D, 143:1-20, 2000. doi:10.1016/S01167-2789(00)00094-4.

[8] Mark Panaggio and Daniel Abrams. *Chimera states: Coexistence of coherence and incoherence in networks of coupled oscillators.* Nonlinearity, 28(3), 2015. doi:10.1088/0951-7715/28/3/R67.

Appendix:
Numerical Integration Routine

The initial conditions for each subpopulation are obtained by first using interpolating functions to approximately invert the cumulative distribution function derived from considering the PKD to be a probability distribution function Then the i^{th} oscillator is assigned an initial phase by evaluating the inverted cdf at $\frac{2i-1}{2N_\sigma}$, where N_σ is the size of the corresponding population.

```
nsteps = 100000;
prec = 12;
n1 = 128;
n2 = 128;
tt = 3000;
\[Rho]1 = .75;
\[Rho]2 = .75;
\[Psi]0 = 0;
\[Phi]1 = Random[]*2*Pi;
\[Phi]2 = \[Phi]1 - \[Psi]0;
(*\[Lambda]=\[Mu]/\[Nu]*)
\[Lambda] = 3/4;
\[Alpha] = Pi/2;
PKD = (1 - \[Rho]^2)/(2*
     Pi*(1 + \[Rho]^2 - 2*\[Rho]*Cos[\[Theta] - \[Phi]]));
If[\[Rho]1 != 1,
```

```
 pdf1 = PKD /. {\[Rho] -> \[Rho]1, \[Phi] -> \[Phi]1};,
 pdf1 = DiracDelta[\[Theta] - \[Phi]1];]
If[\[Rho]2 != 1,
 pdf2 = PKD /. {\[Rho] -> \[Rho]2, \[Phi] -> \[Phi]2};,
 pdf2 = DiracDelta[\[Theta] - \[Phi]2];]
If[\[Rho]1 != 1,
 grid1 = Table[2*(i - 1)*Pi/(5*n1 - 1) - Pi, {i, 5*n1}];
 cdf1 = Interpolation[
   Thread[{grid1,
     Table[NIntegrate[pdf1, {\[Theta], -Pi, grid1[[i]]}], {i,
       5*n1}]}]];
 cdf1inv = InverseFunction[cdf1];,
 cdf1[\[Theta]_] :=
  Piecewise[{{0, -Pi <= \[Theta] < \[Phi]1}, {0, \[Phi]1 < \[Theta] \
<= Pi}, {1, \[Theta] == \[Phi]1}}]; cdf1inv[p_] := \[Phi]1;]
If[\[Rho]2 != 1,
 grid2 = Table[2*(i - 1)*Pi/(5*n2 - 1) - Pi, {i, 5*n2}];
 cdf2 = Interpolation[
   Thread[{grid2,
     Table[NIntegrate[pdf2, {\[Theta], -Pi, grid2[[i]]}], {i,
       5*n2}]}]];
 cdf2inv = InverseFunction[cdf2];,
 cdf2[\[Theta]_] :=
  Piecewise[{{0, -Pi <= \[Theta] < \[Phi]2}, {0, \[Phi]2 < \[Theta] \
<= Pi}, {1, \[Theta] == \[Phi]2}}]; cdf2inv[p_] := \[Phi]2;]
ps1 = Table[(2*i - 1)/(2*n1), {i, n1}];
seeds1 = Table[cdf1inv[ps1[[i]]], {i, n1}];
ps2 = Table[(2*i - 1)/(2*n2), {i, n2}];
seeds2 = Table[cdf2inv[ps2[[i]]], {i, n2}];
seeds = Join[Table[y[i][0] == seeds1[[i]], {i, n1}],
   Table[y[i + n1][0] == seeds2[[i]], {i, n2}]];
seeds0 = Join[seeds1, seeds2];
```

```
Kinter = 1;
Kintra = \[Lambda];
(K1 = Table[Kintra/n1, {i, n1}, {j, n1}]) // MatrixForm;
(K2 = Table[Kinter/n2, {i, n1}, {j, n2}]) // MatrixForm;
(K3 = Table[Kinter/n1, {i, n2}, {j, n1}]) // MatrixForm;
(K4 = Table[Kintra/n2, {i, n2}, {j, n2}]) // MatrixForm;
(K = ArrayFlatten[{{K1, K2}, {K3, K4}}]) // MatrixForm;
eqn = Join[
   Table[y[i]'[t] ==
     Sum[K[[i]][[j]]*Sin[y[j][t] - y[i][t] - \[Alpha]], {j,
       n1 + n2}], {i, n1 + n2}], seeds];
g = Table[y[i][t], {i, n1 + n2}] /.
   NDSolve[eqn, Table[y[i], {i, n1 + n2}], {t, 0, tt},
    MaxSteps -> nsteps, PrecisionGoal -> prec, AccuracyGoal -> prec];
ord1 = Sum[Exp[I*g[[1]][[i]]], {i, n1}]/n1;
ord2 = Sum[Exp[I*g[[1]][[i]]], {i, n1 + 1, n1 + n2}]/n2;
r1 = Abs[ord1];
r2 = Abs[ord2];
phi1 = Arg[ord1];
phi2 = Arg[ord2];
```

g then is a list of interpolating functions of time, one for each oscillator, with domain $t \in [0, tt]$.